ACS Chemical Neuroscience

Research Article

pubs.acs.org/chemneuro

De Novo Design of Self-Assembled Hexapeptides as β-Amyloid (Aβ) Peptide Inhibitors

Qiuming Wang,[†,⊥] Guizhao Liang,[§,⊥] Mingzhen Zhang,[†] Jun Zhao,[†] Kunal Patel,[‡] Xiang Yu,[†] Chao Zhao,[†] Binrong Ding,[∥] Ge Zhang,[‡] Feimeng Zhou,*[,∥] and Jie Zheng*[,†]

[†]Department of Chemical and Biomolecular Engineering and [‡]Department of Biomedical Engineering, The University of Akron, Akron, Ohio 44325, United States

[§]Key laboratory of Biorheological Science and Technology, Ministry of Education College, Chongqing University, Chongqing 400044, China

[∥]Department of Chemistry and Biochemistry, California State University, Los Angeles, California, 90032, United States

Supporting Information

ABSTRACT: The ability of peptides to construct specific secondary structures provides a useful function for biomaterial design that cannot be achieved with traditional organic molecules and polymers. Inhibition of amyloid formation is a promising therapeutic approach for the treatment of neurodegenerative diseases. Existing peptide-based inhibitors are mainly derived from original amyloid sequences, which have very limited sequence diversity and activity. It is highly desirable to explore other peptide-based inhibitors that are not directly derived from amyloid sequences. Here, we develop a hybrid high-throughput computational method to efficiently screen and design hexapeptide inhibitors against amyloid-β (Aβ) aggregation and toxicity from the first principle. Computationally screened/designed inhibitors are then validated for their inhibition activity using biophysical experiments. We propose and demonstrate a proof-of-concept of the "like-interacts-like" design principle that the self-assembling peptides are able to interact strongly with conformationally similar motifs of Aβ peptides and to competitively reduce Aβ−Aβ interactions, thus preventing Aβ aggregation and Aβ-induced toxicity. Such a de novo design can also be generally applicable to design new peptide inhibitors against other amyloid diseases, beyond traditional peptide inhibitors with homologous sequences to parent amyloid peptides.

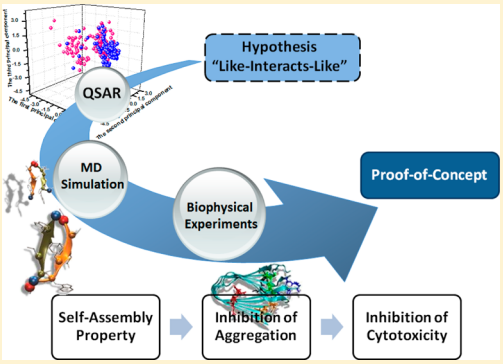

KEYWORDS: *Amyloid inhibitor, protein misfolding, self-assembled peptide, amyloid cytotoxicity, Alzheimer's disease*

The pathology of Alzheimer's disease (AD) is tightly linked to the misfolding and self-aggregation of amyloid-β (Aβ) peptides into extracellular amyloid plaques containing β-structure-rich fibrils in the human brain. Great efforts and progress have been made to develop inhibitors that can (i) block the expression of the amyloid precursor protein (APP), (ii) prevent the proteolytic cleavage of APP into Aβ peptide, or (iii) clear different Aβ aggregates (monomers, oligomers, or fibrils) from the human body.[1−3] However, these strategies have not produced any effective clinical agent to date. In addition to the upstream processes, searching for inhibitors that can inhibit Aβ aggregation would provide alternative therapeutic opportunity for treating AD. Small organic molecules and peptides/peptidomimetics are the two major classes of inhibitors being currently developed for the prevention of Aβ aggregation and Aβ-induced cell toxicity.[4−6]

Peptide-based inhibitors offer several advantages over organic inhibitors: ease of synthesis and sequence/structure modifications, benign biocompatibility, and biomimetic nature. However, the existing peptide-based inhibitors have very limited sequence diversity, because most of them are derived from the central hydrophobic cluster or hydrophobic C-terminal sequences of full-length $A\beta_{1-42}$ such as $A\beta_{15-21}$, $A\beta_{16-22}$, $A\beta_{30-40}$, $A\beta_{34-42}$, and other mutated analogues.[7−9] Since these Aβ fragments are highly homologous to Aβ sequence, it is not surprising that they could interact with the homologous sequence and conformationally similar β-sheet-rich structure of Aβ to mediate the folding and aggregation of Aβ.[10,11] Similar design strategy has often been used to search the entire sequence of other amyloid peptides and to identify peptide fragments, which have the potential to inhibit the aggregation of the parent amyloid peptides. A number of fragmental inhibitors have been found to inhibit their parent amyloid peptides of α-synuclein,[12] human islet amyloid polypeptide (hIAPP),[13−16] serum amyloid protein,[17] and β_2-microglobulin.[18] Interestingly, some peptide fragmental inhibitors can also independently form amyloid fibrils with similar structural morphologies to those formed by their parent

Received: July 30, 2014
Revised: August 15, 2014
Published: August 18, 2014

peptides. To a broader extent, recent studies have shown that the cross-sequence interaction between different amyloid peptides was observed between Aβ-tau,[19,20] Aβ-hIAPP,[21−23] Aβ-transthyretin,[24] α-synuclein-tau,[25,26] tauK18-tauK19,[27,28] human IAPP-rat IAPP,[29,30] SEVI-PAP248−286,[31] α-synuclein-insulin,[32] and IAPP-insulin.[33−35] Some of cross-sequence interactions promote amyloid aggregation, while others do not. This may imply that the cross-sequence interaction could be governed by conformational selection of compatible states between different amyloid peptides. If the dominant conformations of two amyloid sequences are similar, they can interact with each other.[36] While the molecular mechanisms of peptide-based inhibitors against amyloid folding and aggregation have not been clearly understood due to its complexity, these studies of cross-sequence interactions between different amyloid peptides seem to suggest that both homologous and heterogeneous amyloid sequences, as long as they possess similar β-sheet-rich conformations, can interact with each other via the conformational selection (i.e., "like-interacts-like") mechanism, which in turn modulates amyloid aggregation under certain conditions. Therefore, it is possible to search for peptide inhibitors that do not necessarily have homologous sequences to their parent amyloid peptides.[37,38]

Considering that all amyloid peptides exhibit strong self-aggregation ability and share common β-sheet structural characteristics, we proposed a "like-interacts-like" hypothesis to design peptide-based amyloid inhibitors: if computationally designed peptides exhibit strong self-aggregation ability to form β-structure-rich aggregates, these peptides are likely to interact strongly with structurally similar motifs of Aβ peptides and to competitively reduce Aβ-Aβ interactions, leading to the prevention of Aβ aggregation.[37,39−41] Herein, we combined bioinformatics model, molecular dynamics (MD) simulations, and in vitro experiments to test design principle for designing new peptide-based inhibitors in a large-scale of sequence space, which are not derived from Aβ sequence. We developed a cost-effective, high-throughput screening QSAR (quantitative structure−activity relationship) method to establish a sequence−structure−activity relationship of the available peptide inhibitors in database, and then applied the QSAR model to select the representative inhibitor sequences to test our design principle. MD simulations were used to determine the self-aggregation ability, structural characteristics, and interaction modes of β-sheet formation of designed peptide inhibitors. The inhibition capacity of the designed peptide inhibitors against Aβ aggregation and Aβ-induced cell toxicity was further validated using ThT, CD, AFM, SPR, and cell assay. This work provides a new structure-based design principle for the design of heterogeneous peptide-based amyloid inhibitors beyond traditional homologous peptide inhibitors that are directly derived from Aβ sequence.

RESULTS AND DISCUSSION

Computational Design and Screen of Amyloidogenic Hexapeptides. To test our design hypothesis, we developed a structure-based "Index of Natural and Non-natural Amino Acids" (NNAAIndex) QSAR model to high-throughput screen and identify new amyloidogenic hexapeptides as potential Aβ inhibitors. Briefly, the NNAAIndex was able to characterize a total of 335 physicochemical and other properties for 20 natural and 593 non-natural amino acids, followed by clustering these 335 properties into 6 fingerprint factors, that is, hydrophobicity, alpha and turn propensity, bulky property, local flexibility, compositional characteristics, and electronic property. Based on fingerprint factor scores for each amino acid, the NNAAIndex method can represent sequence and structural features of any peptide or peptidomimetics by simply constructing $6 \times n$ matrices (n is the number of residues). We have successfully applied the NNAAIndex-QSAR method to high-throughput screen and design (non)natural peptides of bitter tasting dipeptides, angiotensin-converting enzyme inhibitors, and silica-binding peptides.[42]

Here, we first used two experimentally verified amyloidogenic hexapeptide databases (the Waltz database[43] and the AmylHex database[44,45] containing a total of 278 hexapeptide sequences) as an initial training data set to construct a NNAAIndex model. Then, we combined the NNAAIndex model with linear discriminant analysis (LDA) method to screen, design, and identify 8000 new peptides with predictable self-assembling activity (positive discriminant score, denoted as +) and an additional 30 000+ peptides with non-self-assembling activity (negative discriminant score, denoted as −). The hexapeptides(+) are completely different from any fragmental sequence of Aβ, but they are capable of self-assembling into amyloid-like aggregates and fibrils. Some representative hexapeptides are listed in Table S1 in the Supporting Information. The validity and self-consistency of the QSAR model were assessed by the leave-one-out cross-validation, resulting in predictive accuracy of 71.94%, sensitivity of 75.86%, specificity of 69.14%, and area under the receiver operating characteristic curve of 0.725 (Supporting Information Figures S1−S4). This confirms that the NNAAIndex-QSAR yields satisfactory external predictive ability. The detailed QSAR algorithms, model description, analysis methods, and statistical results and interpretation are provided in the Supporting Information (Figures S1−S6).

Figure 1 shows the position preference of specific amino acids with different fingerprint properties that control the self-assembling ability of the designed hexapeptides. It is clear that some amino acid positions at 1, 3, 4, and 5 are more crucial, as amino acid residues in these positions can be substituted to improve self-assembling ability. Interestingly, for modulation of the hydrophobicity and steric hindrance, we found that only a slight preference of hydrophobic and bulky properties of the residues at 1, 3, 5 and 4, 5 positions was detected, respectively. Balancing with other physical properties such as local flexibility, it appears that the sequence composition is more important for improving self-assembling ability, and this finding is similar to those works by Eisenberg et al. and Rousseau et al.[43,45] Further

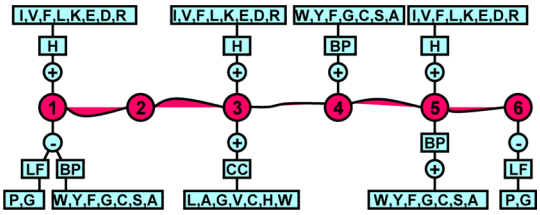

Figure 1. (Dis)favored amino acids at different positions with six fingerprint factors for controlling self-assembling properties of hexapeptides. Amino acids are represented by single letters. The "+" and "−" represent positive and negative contributions to the discriminant scores, respectively. H (hydrophobicity), BP (bulky properties), LF (local flexibility), and CC (compositional characteristics).

dx.doi.org/10.1021/cn500165s | ACS Chem. Neurosci. 2014, 5, 972−981

analysis of the effects of six fingerprint properties at different positions between self-assembling and non-self-assembling sequences revealed obvious differences in the hydrophobicity of the third, fourth, and fifth positions, the alpha and turn propensities of the first, third, and fifth positions, the bulky properties of the first, fourth, and fifth positions, and the compositional characteristics and electronic properties of the third and fifth positions (Figure S5). While the NNAAIndex-QSAR model enables one to high-throughput screen a huge sequence space and to establish the correlation of peptide quantifiable properties (descriptors) with self-assembling properties. But this model does not necessarily attempt to directly and truly determine self-assembling peptides due to the lack of 3D structures of peptides, atomic interactions between and within peptides, and environmental effects. Thus, of the 8000 sequences with self-assembling propensity predicted by QSAR, we randomly selected 35 hexapeptides with the predictive high, moderate, and low self-assembling ability as indicated by discriminant scores to examine their self-assembling properties and structural features using atomistic MD simulations and experiments (Table S1). The selected hexapeptides are highly hydrophobic, but still contain at least one polar residue and one spacer residue to enhance their water solubility.

MD Simulations of Self-Assembling Property of Amyloidogenic Hexapeptides. Given that dimer is a basic building block for any large self-assembling aggregate, we performed all-atom explicit-water MD simulations to examine the structural stability of 35 designed hexapeptide dimers (Table S1), with two typical peptide organizations (parallel and antiparallel orientation relative to each other) using the NAMD program[46] and the CHARMM27 force fields.[47] A dimer was constructed by packing two peptides, each adopting a β-strand conformation, on the top of each other in either a parallel or antiparallel manner, with an initial peptide−peptide separation distance of ∼4.7 Å. Such a conformation corresponds to the characteristic X-ray scattering diffraction signal of interstrand distance in β-sheets of amyloid fibrils. MD trajectories showed that 11 out of 35 peptide dimers exhibited relative high structural stability (the data in Figure 2 show the structurally unstable sequence of PTRCGP as a negative control). Figure S7 shows the backbone RMSD of hexapeptide dimers with parallel and antiparallel peptide organizations, demonstrating the structural stability of self-assembling hexapeptides during 20 ns simulations. With the parallel organization, except for CTIYWG(+) and PTRCGP(−) which tend to disassociate with each other, the other 10 hexapeptides(+) were able to retain high β-sheet contents (66%−85%) with an averaged interpeptide distance of 5.4−6.7 Å (Figure 2A). Interestingly, GTVWWG(+) changed its initial parallel organization into antiparallel one, while still remaining tight interpeptide association and stable β-sheet structure afterward. Consistent with parallel models, Figure 2B shows that most of the stable parallel dimers can also retain the stable antiparallel orientation with strong peptide association with the following exceptions: (i) ITLFWG(+) exhibited unstable (stable) structure in antiparallel (parallel) packing; (ii) PTRCGP(−) as a negative control lost 90% of native contacts and initial ordered structure for both parallel and antiparallel organizations; (iii) GTVWWG(+) was quite stable with a preferable antiparallel packing, consistent with orientation change from parallel orientations; and (iv) CTIYWG(+) tended to adopt a stable, antiparallel structure over an unstable parallel structure. Our

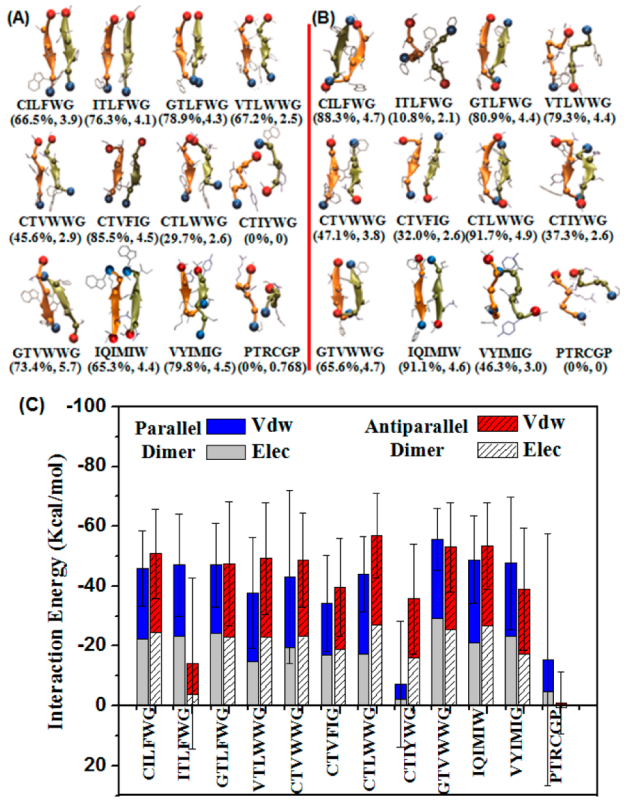

Figure 2. Structural and energetic characteristics for hexapeptide dimers. MD snapshots of hexapeptide dimers with (A) parallel and (B) antiparallel peptide organizations. β-Sheet percentage and number of hydrogen bonds of hexapeptide dimers are listed in parentheses. (C) Averaged nonbonded interaction energy between two adjacent peptides of dimers. There is a reasonable positive correlation between β-sheet content/the number of hydrogen bonds and interpeptide interactions between peptides.

MD results not only confirm the designs by QSAR method, but also suggest mixed dimers with both parallel and antiparallel conformations coexist in fibers.

A secondary structural analysis also confirmed that regardless of parallel or antiparallel packing, most of stable dimers retain a high content of the β-structure more than 65% (Figures 2 and S8A). A large population of the β-sheet structure was inherent to hydrogen bonding between dimeric peptides. For stable dimers, hydrogen bonds between adjacent peptides are almost evenly distributed along the two β-strand directions throughout the simulations. Once formed, these hydrogen bonds of ∼4+ pairs are rarely broken and act as a zipper to retain the (anti)parallel interchain organization (Figures 2A,B and S8B). Some short peptides have been computationally identified to amyloid-like fibrils via self-complementary, steric zippers between β-sheets.[45] To more precisely interpret the structural stability of dimers, we calculated nonbonded interactions between peptides that account for all different contributions from hydrogen bonding, hydrophobic interaction, $\pi-\pi$ stacking, and other side chain contacts. Figure 2C shows that, of nine stable dimers depicted, the change of the relative orientation of these peptides from parallel to antiparallel did not cause a large change of favorable interpeptide interactions, with a small range of energy differences of 1.1−13.4%. Decomposition the interpeptide interaction energies into the van der Waals (VDW) and electrostatic contributions further revealed that irrespective of peptide sequence and orientation,

dx.doi.org/10.1021/cn500165s | ACS Chem. Neurosci. 2014, 5, 972−981

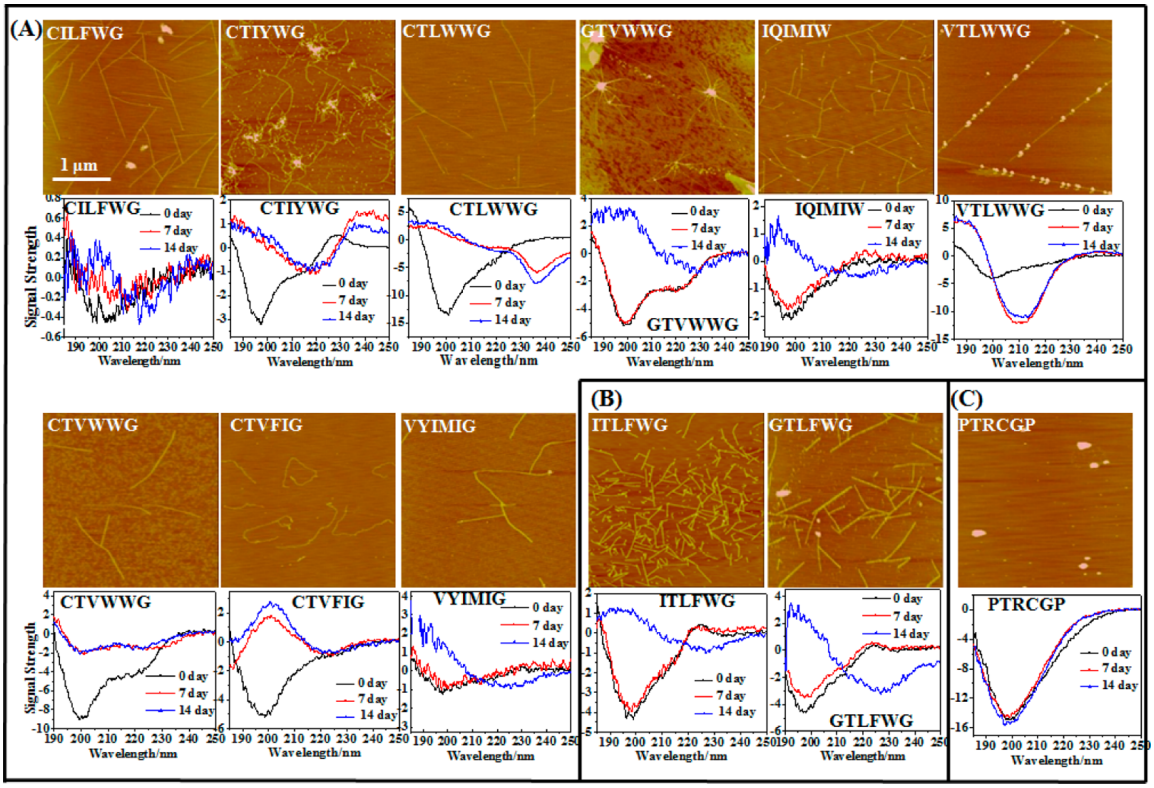

Figure 3. Formation of amyloid-like fibrils by the computationally designed hexapeptides monitored using AFM (upper panel) and CD (lower panel). The hexapeptides are classified into three groups with (A) high, (B) moderate, and (C) low or no self-assembling property. Hexapeptides (2 mM) were incubated in phosphate buffer solution at 37 °C for 2 weeks.

VDW interaction is comparable to electrostatic interaction (Figure 2C), suggesting that peptide association is in a cooperative mode. Some peptides (e.g., ITLFWG, VTLWWG, CTLWWG, and CTIYWG) showed notable difference in electrostatic interactions between parallel and antiparallel models.

Experimental Assessment of Computationally Designed Hexapetides for Fibrillation. To validate the designs by QSAR model and MD simulations, we examined whether these designed peptides can self-assemble into amyloid-like fibrils containing the typical β-sheet structure using atomic force microscopy (AFM) and circular dichroism (CD). AFM images (Figure 3) clearly showed that, upon incubation of 11 hexapeptides(+) at 2 mM in PBS solution, all peptides(+) exhibited amyloidogenic propensity to some degrees. Nine peptides (CILFWG, CTIYWG, CTLWWG, GTVWWG, IQIMIW, VTLWWG, CTVWWG, CTVFIG, and VYIMIG) formed long and thick amyloid-like fibers with diameters of 5−15 nm and lengths of $\geq$1 μm, while two peptides (ITLFWG and GTLFWG) formed a few very short and broken fibers ($\leq$1 μm) and exhibited moderate amyloidogenic propensity. In contrast, the non-amyloid-forming PTRCGP(−) does not form any fibrillar-like aggregate, but instead amorphous aggregates with diameters up to 22 nm. CD spectra juxtaposed below corresponding AFM images in Figure 3 showed that all of the freshly prepared hexapeptides initially adopt a random coil conformation at the very beginning of incubation (cf. the large and deep minimum at ~197 nm). GTVWWG(+), CTIYWG-(+), and CTVWWG(+) also displayed a second, small minimum at ~220 nm, suggesting a mixed β-strand/turn conformation. Upon a 2 week incubation, all of the hexapeptides(+) clearly underwent conformational transition to the β-sheet-rich structures, as indicated by a large maximum value at ~197 nm and a minor minimum value at ~222 nm. As expected, PTRCGP(−) does not show any spectral shift over time, which is indicative of the absence of any β-structure. Our AFM and CD results confirmed the self-aggregation ability predicted by QSAR model and MD simulations. Therefore, the combination of these two computational methods enabled us to develop a cost-effective, high-throughput design/screen of new amyloid-forming peptides from a large pool of sequences.

Experimental Examination of the "Like-Interacts-Like" Model between Aβ and Hexapeptides. We further tested our "like-interacts-like" model by investigating whether the designed self-assembling peptides could competitively interact with conformationally similar amyloid peptides, thereby inhibiting Aβ misfolding and self-assembly. We first examined the inhibitory effect of the designed hexapeptides on Aβ aggregation. The aggregation kinetics and morphological changes of Aβ amyloid formation in the absence and presence of different hexapeptides were monitored by ThT fluorescence assay (Figures 4A and S9A) and AFM (Figures 4B and S9B). In the absence of hexapeptides, increased ThT signals along a typical sigmoid curve and AFM images clearly demonstrated that Aβ monomers aggregated into long and branched amyloid fibrils, with average heights of 8−12 nm and lengths of 1−2.5 μm. Upon coincubation of Aβ (20 μM) with different hexapeptides (40 μM) at 37 °C for 8 h, we observed different Aβ aggregation behaviors. First, CTIYWG(+), CTLWWG(+), and GTVWWG(+) strongly inhibited Aβ aggregation and oligomerization, as evidenced by the significantly reduced ThT signals by 72.3, 99.7, and 87.1% for CTIYWG(+), CTLWWG-(+), and GTVWWG(+), respectively (Figure 4A). AFM images (Figure 4B) consistently showed that Aβ fibril growth was

dx.doi.org/10.1021/cn500165s | ACS Chem. Neurosci. 2014, 5, 972−981

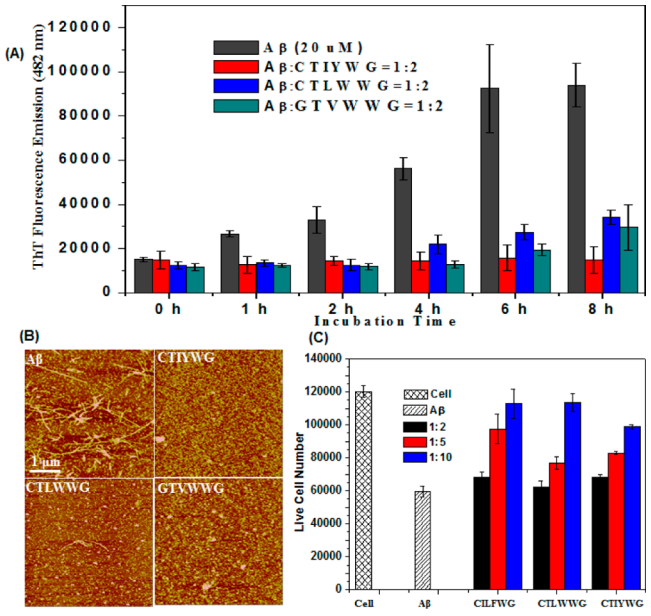

Figure 4. Inhibition of $A\beta_{1-42}$ aggregation and cytotoxicity by self-assembling hexapeptides. (A) Time-dependent ThT fluorescence curves for pure $A\beta_{1-42}$ (20 μM) and mixed Aβ-hexapeptides at molar ratio of 1:2. (B) AFM images for pure $A\beta_{1-42}$ and mixed Aβ-hexapeptides aggregates at 8 h. (C) Inhibition of Aβ-induced cytotoxicity against SH-SY5Y neuronal cells by hexapeptides using MTT assay. Error bars represent the average of five replicate experiments.

arrested, with small amorphous-like aggregates of ~6−12 nm in the presence of CTIYWG(+) and GTVWWG(+), and very few thin protofibrils (~5−10 nm in height and ~100 nm for length) with CTLWWG(+) present. These results indicate that these three hexapeptides are able to bind strongly to Aβ monomers and other aggregation intermediates to halt the structural transition and peptide association of Aβ monomers toward fibrils. Second, CTVFIG(+) and IQIMIG(+) promoted Aβ aggregation. Within the first 2 h, the structural transition was similar to that of pure Aβ solution (Figure S9A). The structural transition was accelerated after 4 h incubation since the ThT signal displayed an increase of 41.9% for the Aβ/CTVIFG(+) mixture and 13.3% for the Aβ/IQIMIW(+) mixture. AFM images showed many thicker mature fibrils produced in the presence of these two hexapeptides (Figure S9B). The enhanced Aβ aggregation could be due to that these hexapeptides preferentially accelerate fibril formation by consuming conformational rate limiting Aβ oligomers. Finally, CILFWG (+), GTLFWG(+), and PTRCGP(−) displayed either weak or no inhibition effect on Aβ aggregation, as indicated by the ThT and AFM results (Figure S9). Additionally, since all selected hexapeptides(+) exhibit amyloid characteristics, different hexapeptide-induced inhibition and promotion of Aβ fibril formation could be due to a complicated conformational selection of compatible (complementary) states between different species.[36]

To further confirm specific binding behaviors between designed peptides and Aβ, we performed SPR experiments to determine binding affinities between hexapeptides and Aβ (Figure 5). K_D was obtained from Figure 5A using a monovalent binding model to best fit binding curves at equilibrium. The negative control PTRCGP(−) bound to Aβ with a K_D of 169.7 ± 51.8 μM, suggesting a very weak Aβ−ligand interaction. Among 11 self-assembling hexapeptides(+), 6 hexapeptides displayed strong binding affinity to Aβ as evidenced by K_D ranging from 0.841 ± 0.078 to 4.421 ± 1.624

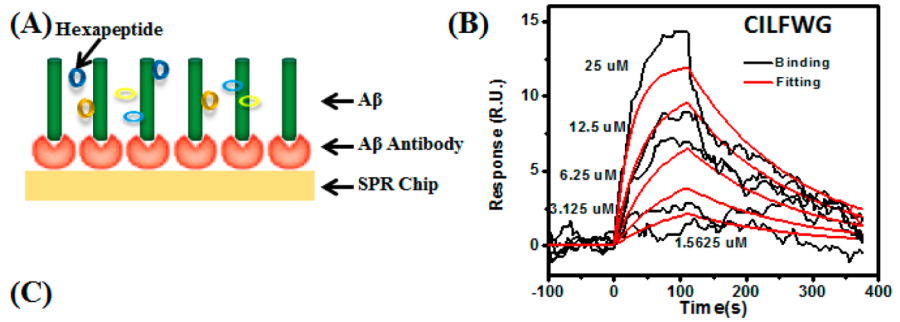

(C)

	I (Strong Binding)		
Hexapeptide	GTVWWG	CILFWG	CTIYWG
K_D (μM)	0.841 ± 0.078	3.023 ± 1.415	1.724 ± 0.519
Hexapeptide	IQIMIW	CTVFIG	CTVWWG
K_D (μM)	3.274 ± 1.261	4.421 ± 1.624	2.486 ± 1.399

	II (Moderate Binding)	
Hexapeptide	VTLWWG	CTLWWG
K_D (μM)	10.809 ± 2.546	36.116 ± 7.136

	III (Weak Binding)			
Hexapeptide	ITLFWG	GTLFWG	VYIMIG	PTRCGP
K_D (μM)	140.022 ± 14.657	148.115 ± 19.359	180.618 ± 40.493	169.663 ± 51.803

Figure 5. Validation of binding between $A\beta_{1-42}$ and hexapeptide by SPR. (A) Scheme of hexapeptide binding assay on $A\beta_{1-42}$ functionalized SPR gold surface. (B) Representative set of binding data for CILFWG with determination of molecular binding constants by fitting the SPR binding data (black) with theoretical models (red). Five runs are overlaid for concentrations at 25, 12.5, 6.25, 3.125, and 1.5625 μM. (C) Dissociation constant (KD) of hexapeptides with $A\beta_{1-42}$ monomer.

dx.doi.org/10.1021/cn500165s | ACS Chem. Neurosci. 2014, 5, 972−981

μM, two of them showed moderate binding affinity (K_D ranges from 10.809 ± 2.546 to 36.116 ± 7.136 μM), and three of them (VYIMIG, ITLFWG, and GTLFWG) showed weak binding affinity (K_D is larger than 120 μM). Our SPR results confirm that the inhibitory ability of self-assembling peptides to largely suppress Aβ aggregation arises from their strong binding affinity to Aβ. Particularly, these peptides bind to Aβ monomers relatively strongly ($\leq$40 μM). Consequently, association of these peptide inhibitors to the secondary structure of Aβ would suppress Aβ aggregation and inhibit Aβ toxicity. The ligand with greater binding affinity to Aβ is often found to effectively inhibit Aβ aggregation and cytotoxicity.[48]

A sequence analysis of 182 designed hexapeptides with strong self-assembling property showed that Cys, Val, Trp, Phe, and Ile are frequently occurring hydrophobic residues, while charged residues of Asp, Lys, Glu, and Arg have the lowest (Figure S6). This because in the typical, parallel β-sheets electrostatic repulsion arisen from charge−charge stacking disfavors the self-aggregation of peptides, thus requiring additional stronger stabilizing forces to compensate such repulsive forces. Gly was found to facilitate the α-helix to β-sheet transition and function as a molecular notch to stabilize the sheet-to-sheet packing in amyloids due to the lack of side chain chirality. Cys and Thr are likely to increase the intersheet electrostatic interactions, strengthening the association of the peptide inhibitors with amyloid motifs.

Experimental Affirmation of Hexapeptide Reduce Aβ-Induced Cell Toxicity. Having demonstrated that the designed hexapeptides can interact with Aβ and inhibit Aβ aggregation, we examined whether the hexapeptides can protect neuronal cells from Aβ-induced toxicity using the MTT SH-SY5Y cell assay with fixed concentration of Aβ (20 μM) in the presence of different Aβ/hexapeptide molar ratios of 1:2, 1:5, and 1:10. MTT results (Figures 4C and S10) show that incubation of Aβ (20 μM, pH 7.4) alone for 24 h led to ∼50% cell viability, indicating that Aβ is highly toxic to cells as expected. As a positive control, coincubation of hexapeptides and the SH-SY5Y cells demonstrated that these hexapeptides themselves had almost no or low cytotoxicity, with cell viability of 81%−122% (Figure S10A). When SH-SY5Y cells were exposed to mixtures of Aβ and hexapeptides, five hexapeptides (CILFWG, CTLWWG, CTIYWG, IQIMIW, and VYIMIG) exhibited a dose-dependent increase in cell viability as peptide concentrations, while the other seven hexapeptides (GTVWWG, CTVFIG, VTLWWG, ITLFWG, GTLFWG, CTVWWG, and PTRCGP) were almost inactive at different doses tested (Figures 4C and S10B). At a lower Aβ:hexapeptide ratio of 1:2, almost all hexapeptide did not significantly reduce Aβ-induced toxicity. Cell viability only improved by 2.1−14.6% as compared to cells exposed to pure Aβ. However, as the Aβ/hexapeptide ratio increased to 1:5, five hexapeptides increased cell viability up to ∼31.7%. More significantly, at the Aβ/hexapeptide of 1:10, CILFWG(+), CTLWWG(+), and CTIYWG(+) strongly suppressed the Aβ-induced cell death, Aβ cytotoxicity was almost completely inhibited, and cell viability was improved by 32.6−45.1% relative to Aβ-induced cell death, leading to overall cell viability of 82.1−94.6%. Considering that the designed hexapeptide inhibitors themselves had little or rather weak cytotoxicity to neuronal cells, at the higher Aβ:hexapeptide ratios (>1:5) the hexapeptides enable to more effectively sequester Aβ aggregates, which help to convert toxic Aβ oligomers into nontoxic or less toxic Aβ-inhibitor complexes, leading to the protection of cells from toxic Aβ aggregates. Although not all self-assembling hexapeptides can protect cells from Aβ-induced cytotoxicity, we indeed discovered several new peptide sequences with dual functionalities of self-assembling and Aβ inhibition properties. Our de novo computational design offers a great feasibility and flexibility to develop new peptide inhibitors of Aβ that are not derived from Aβ sequence.

CONCLUSIONS

In conclusion, we combine a QSAR model, MD simulations, and biophysical experiments to systematically and efficiently screen/design, characterize, and identify a series of self-assembling hexapeptides as potential Aβ inhibitors. Particularly, these new sequences are not directly derived from amyloid sequences. The collective computational and experimental results demonstrate a proof-of-concept of the "like-interacts-like" design principle that self-assembling peptides with amyloidogenic properties are able to interact strongly with conformationally similar motifs of Aβ peptides and to competitively reduce Aβ−Aβ interactions, thus preventing Aβ aggregation and Aβ-induced toxicity. More importantly, due to common structural and aggregation characteristics of amyloid peptides, the designed peptide-based inhibitors are also likely to prevent other amyloid peptide aggregation. These new sequences can serve as a selection pool to be used as amyloid inhibitors with further structural modification by non-natural amino acids for improving their inhibitory ability against amyloid diseases, or as self-assembling materials with well-defined β-sheet structures for other biological applications.

METHODS

QSAR Modeling and Analysis. *Structural Representation.* The QSAR model is built on two data sets of the Waltz data set[49] and the AmylHex data set,[44] consisting of 116 positive amyloid-forming peptides and 162 negative non-amyloid-forming peptides. We developed and applied the "Index of Natural and Non-natural Amino Acids" (NNAAIndex) QSAR model to characterize the structural features of a total of 278 training hexapeptides as follows: we first determined 335 physicochemical properties (e.g., alpha and turn propensities, beta propensity, composition, hydrophobicity, physicochemical properties, and other properties) to characterize the structural features of 20 natural and 593 non-natural amino acids. Then, we used a principal component method with a Kaiser normalized Promax algorithm to cluster 335 properties into 6 new NNAAIndex fingerprint factors, including hydrophobicity, alpha and turn propensities, bulky properties, compositional characteristics, local flexibility, and electronic properties, which account for 83.5% variance of 335 properties based on the relationship between components and eigenvalues. Since each amino acid is represented by 6 NNAAIndex factors, the structural features of any hexapeptide designed/used in this study can be readily characterized by simply constructing a 6 × 6 NNAAIndex matrix.

Correlation Methods. A linear discriminant analysis (LDA) was used to classify the dependence of the hexapeptides using $Y = a_0 + a_1X_1 + a_2X_2 + ... + a_nX_n$, where Y is a dependent variable; X_1, X_2,... X_n represents the independent variables (observed values); discriminant coefficients of a_1, a_2, ... a_n correspond to the weights associated with the respective independent variables. A hyperplane defined by the linear discriminant function was applied to divide a n-dimensional descriptor space into two classes (two regions), in which each hexapeptide was discriminated into one of two classes. The predictive classification of each sample was determined by the predictive scores derived from the LDA model. The variables as inputs in the model were selected by a stepwise method to decrease the number of descriptors and to make the model more interpretable. The selection of the variables was based on F value of the partial F test: the variable

was accepted by the model if F value was larger than 3.84, while it was rejected if F value was less than 2.71.

Model Validation. The predictive performance of the QSAR model was validated using a jackknife test (leave-one-out, LOO, cross-validation). In the LOO test, to avoid any biased propensity by using single randomly selected sample in the data set, 278 samples were iteratively removed one at a time (i.e., one removed sample as a predicted sample, while the remaining samples as training samples), and the predictive performance was recalculated each time and then averaged by 278 times.[50] A variety of statistical assessments including accuracy (Acc), sensitivity (S_n), specificity (S_p), and the area under the receiver operating characteristic (ROC) curve (AUC) were also used to evaluate the performance of the QSAR model. Acc calculated the percentage of samples that were correctly identified. S_n measured the ability to correctly predict amyloid-forming peptides, while S_p measured the ability to correctly reject nonamyloid-forming peptides. S_n and S_p were threshold dependent measurements, so they failed to present all the information provided by one predictive method. Thus, the AUC, a trade-off between S_n and S_p, which was another threshold independent measure, was used to assess the modeling performance.

MD Simulations of Hexapeptide Aggregation. To examine the self-association ability of the designed hexapeptides, we constructed two different flat β-sheet structures using two copies of the same hexapeptides, with a parallel or antiparallel orientation of two peptides relative to each other. Considering that a dimer is the smallest building block of the large peptide aggregates, each peptide was packed parallel (antiparallel) on the top of the other and no translation was applied to one peptide relative to the other. The initial interpeptide distance was set to 4.7 Å corresponding to a characteristic X-ray scattering diffraction value within a β-sheet structure.[51] Both C- and N-termini of each peptide were not capped by carboxyl and amine groups in order to avoid the potential artifact electrostatic repulsion and attraction in both parallel and antiparallel models.

MD simulations were performed using the NAMD software[46] with CHARMM27 force field.[47] Each model system was solvated in a pre-equilibrated box of TIP3P water molecules, with a margin of at least 10 Å from any edge of the water box to any hexapeptide atoms. Each system was then neutralized by adding Cl^- and Na^+ ions to mimic an ionic strength of 100 mM. The resulting systems were subjected to 5000 steps of steepest decent minimization with peptide backbone atoms harmonically constrained, followed by 5000 additional steps of conjugate gradient minimization without any constraint. Short 1 ns MD simulations were performed to heat the system from 0 to 310 K by constraining the backbones of dimers. The production MD simulations were performed using an isothermal−isochroic ensemble (NPT, where T = 310 K and P = 1 atm) under periodic boundary conditions. All covalent bonds involving hydrogen were constrained by the RATTLE method so that a 2 fs time step was used in the velocity Verlet integration. van der Waals (VDW) interactions were calculated by the switch function with a twin-range cutoff at 12 and 14 Å. Long-range electrostatic interactions were calculated using the force-shifted method with a 14 Å cutoff. Structures were saved every 2 ps for analysis. All analyses were performed using tools within CHARMM, VMD, and codes developed in-house.

Experimental Methods. *Materials.* Hexapeptides (>95% purity) were synthesized by Selleckchem Inc. (Houston, TX). Aβ_{1-42} peptide (≥95.5%) was purchased from American Peptide Inc. (Sunnyvale, CA). 1,1,1,3,3,3-Hexafluoro-2-propanol (HFIP, ≥99.9%), dimethyl sulfoxide (DMSO, ≥99.9%), HCl, NaOH, Na_2HPO_4, NaH_2PO_4, phosphate buffer (10 mM, pH = 7.4), thioflavin T (ThT, 98%), Tween 20, Dextran from Leuconostoc spp, and 3-(4,5-dimethylthiazol-2-yl)-2,5-diphenyltetrazolium bromide (MTT, 98%) were purchased from Sigma-Aldrich (St. Louis, MO).

Peptide Pretreatment. Aβ_{1-42} or hexapeptide was purified to obtain a homogeneous solution of monomeric Aβ or hexapeptide with unstructured conformation using our previously established methods.[52,53] Briefly, all hexapeptides and Aβ were dissolved in 1,1,1,3,3,3-hexafluoro-2-propanol (HFIP) for 2 h (1 mg/mL), sonicated for 30 min to remove any preformed aggregates or seeds, and centrifuged at 14 000 rpm for 30 min at 4 °C. The top Aβ- or hexapeptide-HFIP solution was pipetted out, frozen with liquid nitrogen, and dried in a freeze-dryer at −108 °C. The dry hexapeptide or Aβ powder was lyophilized at −80 °C before use.

Self-Aggregation of Hexapeptides. Immediately prior to use, the HFIP-treated and lyophilized hexapeptide powder was predissolved in 10 mM NaOH (final concentration of 5%). Hexapeptide solution was prepared at 2 mM by dissolving the NaOH concentrated hexapeptide solution into 100 mM phosphate buffer solution (PBS, pH = 7.4), sonicated for 30 min to dissemble any preformed nuclei in ice water, and centrifuged at 14 000 rpm for 30 min at 4 °C to condense insoluble materials and small oligomers. The supernatant (∼75% of the top solution) was incubated at 37 °C without further agitation for 2 weeks.

Inhibition of Aβ_{42} Aggregation. Homogeneous Aβ_{1-42} solution was required for Aβ inhibition tests. The purified Aβ powder was aliquoted in DMSO for 1 min and sonicated for 30 s. The initiation of 20 μM Aβ [containing 1% (V/V) DMSO] aggregation in solution was accomplished by adding an aliquot of the concentrated DMSO-Aβ solution to 10 mM PBS buffer (pH = 7.4), followed by immediate vortexing for thorough mixing. Aβ solution was then centrifuged at 14 000 rpm for 30 min at 4 °C to remove any existing oligomers, and 75% of the supernatant was removed for further incubation or inhibition experiments. The pure Aβ solution was incubated at 37 °C as control. For Aβ inhibition experiments, 20 mM hexapeptide (in DMSO) stock solution was dissolved in a freshly prepared Aβ monomer solution to a final concentration of 40 μM. The mixed Aβ-hexapeptide (Aβ/hexapeptide = 1:2) samples were incubated at 37 °C and examined by AFM and ThT fluorescence assay.

Tapping-Mode Atomic Force Microscopy (AFM). Tapping-mode AFM was used to monitor the morphological changes of any aggregates formed in hexapeptide-only solution or mixtures containing Aβ_{1-42} and a given hexapeptide. Aliquots (10 μL) at different incubation times were taken out from incubated solutions and cast onto freshly cleaved mica substrates for 30 s, rinsed three times with 50 μL of deionized water to remove any salt and loosely bonded aggregates, and dried with compressed N_2 for 5 min before AFM imaging. Tapping-mode AFM imaging was performed in air using a Nanoscope III multimode scanning probe microscope (Veeco Corp., Santa Barbara, CA) equipped with a 15 μm E scanner. Commercial Si cantilevers (NanoScinece, Phoenix, AZ) with an elastic modulus of ∼40 N/m were used. All images were acquired as 512 × 512 pixel images at a typical scan rate of 1.0−2.0 Hz with a vertical tip oscillation frequency of 250−350 kHz. Representative AFM images were obtained by scanning two individual samples at six or more different locations of each sample.

Circular Dichroism (CD). CD spectra were collected on a J-810 spectropolarimeter (JASCO Inc.) at room temperature in a quartz cuvette. CD spectroscopy measures both the soluble and dispersed species. The hexapeptide solutions at 0 h, 1 week, and 2 weeks were diluted with water at a hexapeptide solution/DI water ratio of 1:5 and placed into a rectangular quartz cuvette of a 0.1 cm path length. The spectra were scanned between 250 and 185 nm at a 0.5 nm resolution and 50 nm/min scan rate. All spectra were corrected by subtracting the baseline and averaged by three successive scans for each sample. During incubation, large hexapeptide aggregates could sink to the bottom of the cuvette out of the detection window, resulting in a loss of the CD signal. For consistency, before each measurement, the cuvette was thoroughly shaken for better dispersion.

Surface Plasmon Resonance (SPR). Surface plasmon resonance (SPR) was used to determine the binding affinity between Aβ_{1-42} and hexapeptide. The SPR measurements and data analysis were conducted on an BI-SPR 4000 system (Biosensing Instrument Inc., Tempe, AZ) equipped with a dual-channel flow cell and two through-the-handle six-port injection valves. PBS (10 mM), containing 0.005% Tween 20 (PBST, pH = 7.4), was thoroughly degassed for 30 min and used as a carrier solution. The dextran-modified sensor chip was preconditioned prior to immobilization by delivering 10 mM HCl, 50 mM NaOH, and 0.1% (w/v) sodium dedecyl sulfate (SDS, Fisher) at a flow rate of 100 μL/min. The dextran chip was covered with streptavidin via the amine coupling chemistry by flushing the flow

channels with 50 μg/mL streptavidin at 20 μL/min). After a stable baseline had been obtained, biotinyated monoclonal Aβ antibody (Covance, MA) was injected to achieve the highest surface coverage at a flow rate of 10 μL/min. Then 2 μM Aβ solution (2 mM) was injected with a syringe pump. A given hexapeptide solution was injected at a flow rate of 40 μL/min.

Thioflavin T (ThT) Fluorescence Assay. The Aβ_{1-42} aggregation in the presence and absence of hexapeptide inhibitors was monitored by ThT assay. ThT solution (2 mM) was prepared by adding 0.0328 g of ThT powder into 50 mL of DI water. Then 250 μL of the 2 mM ThT solution was further diluted into 50 mL of Tris-buffer (pH = 7.4) to reach a final concentration of 10 μM. At different incubation time points, 5 μL of 20 μM Aβ with or without hexapeptides was put into 250 μL of 10 μM ThT-Tris solution. Fluorescence spectra were obtained using a Fluorolog 3 spectrofluorometer (Horiba Jobin Yvon, Edison, NJ). All measurements were carried out in aqueous solutions using a 0.5 cm × 0.5 cm quartz cuvette. ThT fluorescence emission intensity of each sample was recorded between 460 and 510 nm with an excitation wavelength of 450 nm. Each experiment was repeated in three independent samples.

Cell Culture. All chemicals for cell culture tests were purchased from Life Technologies unless otherwise stated. Human neuroblastoma SH-SY5Y cells (ATCC, Manassas, VA) were cultured in 75 cm^2 T-flasks (Corning) in sterile-filtered Eagle's minimum essential medium and Ham's F-12 medium mixed at a 1:1 ratio containing 10% fetal bovine serum (EMEM, ATCC, Manassas, VA) and 1% penicillin/streptomycin at 37 °C under humidified air containing 5% CO_2. Cells were cultured to confluence and then harvested using 0.25 mg/mL trypsin/EDTA solution (Lonza). Before adding Aβ_{1-42} and a given hexapeptide, cells were resuspended in Opti-MEM reduced serum medium and counted using a hemacytometer. Cells were then plated in a 96-well tissue culture plate with approximately 50 000 cells/well in 100 μL of Opti-MEM reduced serum medium, and allowed to attach for 24 h inside the incubator.

MTT Cell Toxicity Assay. Aβ_{1-42} (20 μM) was added into the SH-SY5Y cell media to study Aβ-inflicted cytotoxicity. Vybrβnt MTT cell proliferation assay was performed (Life Technologies). A solution containing 12 mM MTT was prepared by dissolving 5 mg of MTT in 1 mL of sterile PBS (pH 7.4). To each well, 10 μL of MTT solution was added, and the microplates were further incubated at 37 °C for 4 h to convert MTT into formazan crystals. DMSO (200 μL) was then added to each well, and the microplates incubated for an additional 10 min at 37 °C and mixed thoroughly to dissolve the formazan crystals. Formazan crystal quantification was examined using a Synergy H1 microplate reader (BioTek) at 540 nm. The absorbance of negative control wells was averaged and subtracted from all other samples to eliminate background signals. Sample absorbance was then compared with a standard curve to determine the number of viable cells.

■ ASSOCIATED CONTENT

Ⓢ Supporting Information

Table S1 and Figures S1−S10 as described in the text. This material is available free of charge via the Internet at http://pubs.acs.org.

■ AUTHOR INFORMATION

Corresponding Authors

*Phone: 323-343-2390. E-mail: fzhou@exchange.calstatela.edu.
*Phone: 330-972-2096. E-mail: zhengj@uakron.edu.

Author Contributions

⊥Q.W. and G.L. contributed equally to this work. Q.W., G.L., F.Z., and J.Z. designed research; Q.W., G.L., M.Z., J.Z., K.P., X.Y., C.Z., B.D., and G.Z. performed research; Q.W., G.L., B.D., and M.Z. analyzed data; Q.W., G.L., F.Z., and J.Z. wrote the paper.

Funding

G.L. is thankful for the support from the Natural Science Foundation Project of Chongqing CSTC (cstc2012gg-gjhz10003). J.Z. is thankful for the support from NSF grants (CAREER Award CBET-0952624 and CBET-1158447).

Notes

The authors declare no competing financial interest.

■ ACKNOWLEDGMENTS

Anton computer time was in part provided by the National Center for Multiscale Modeling of Biological Systems (MMBioS) through Grant P41GM103712-S1 from the National Institutes of Health and the Pittsburgh Supercomputing Center (PSC). The Anton machine at PSC was generously made available by D.E. Shaw Research.

■ REFERENCES

(1) Dash, P. K., Moore, A. N., and Orsi, S. A. (2005) Blockade of [gamma]-secretase activity within the hippocampus enhances long-term memory. *Biochem. Biophys. Res. Commun. 338*, 777−782.

(2) Asai, M., Hattori, C., Iwata, N., Saido, T. C., Sasagawa, N., Szabó, B., Hashimoto, Y., Maruyama, K., Tanuma, S.-i., Kiso, Y., and Ishiura, S. (2006) The novel beta-secretase inhibitor KMI-429 reduces amyloid beta peptide production in amyloid precursor protein transgenic and wild-type mice. *J. Neurochemistry 96*, 533−540.

(3) Bacskai, B. J., Kajdasz, S. T., Christie, R. H., Carter, C., Games, D., Seubert, P., Schenk, D., and Hyman, B. T. (2001) Imaging of amyloid-[beta] deposits in brains of living mice permits direct observation of clearance of plaques with immunotherapy. *Nat. Med. 7*, 369−372.

(4) Yamin, G., Ruchala, P., and Teplow, D. B. (2009) A peptide hairpin inhibitor of amyloid beta-protein oligomerization and fibrillogenesis. *Biochemistry 48*, 11329−11331.

(5) Soto, P., Griffin, M. A., and Shea, J.-E. (2007) New insights into the mechanism of alzheimer amyloid-{beta} fibrillogenesis inhibition by N-methylated peptides. *Biophys. J. 93*, 3015−3025.

(6) Diaz, J. C., Simakova, O., Jacobson, K. A., Arispe, N., and Pollard, H. B. (2009) Small molecule blockers of the Alzheimer Aβ calcium channel potently protect neurons from Aβ cytotoxicity. *Proc. Natl. Acad. Sci. U.S.A. 106*, 3348−3353.

(7) Doi, T., Kamioka, S., Shimazu, S., and Takahashi, T. (2008) A synthesis of RGD model cyclic peptide by palladium-catalyzed carbonylative macrolactamization. *Org. Lett. 10*, 817−819.

(8) Fradinger, E. A., Monien, B. H., Urbanc, B., Lomakin, A., Tan, M., Li, H., Spring, S. M., Condron, M. M., Cruz, L., Xie, C. W., Benedek, G. B., and Bitan, G. (2008) C-terminal peptides coassemble into Abeta42 oligomers and protect neurons against Abeta42-induced neurotoxicity. *Proc. Natl. Acad. Sci. U.S.A. 105*, 14175−14180.

(9) Li, H., Monien, B. H., Fradinger, E. A., Urbanc, B., and Bitan, G. (2010) Biophysical characterization of Abeta42 C-terminal fragments: inhibitors of Abeta42 neurotoxicity. *Biochemistry 49*, 1259−1267.

(10) Takahashi, T., and Mihara, H. (2008) Peptide and protein mimetics inhibiting amyloid β-peptide aggregation. *Acc. Chem. Res. 41*, 1309−1318.

(11) Austen, B. M., Paleologou, K. E., Ali, S. A. E., Qureshi, M. M., Allsop, D., and El-Agnaf, O. M. A. (2008) Designing peptide inhibitors for oligomerization and toxicity of Alzheimer's β-amyloid peptide. *Biochemistry 47*, 1984−1992.

(12) El-Agnaf, O. M., Paleologou, K. E., Greer, B., Abogrein, A. M., King, J. E., Salem, S. A., Fullwood, N. J., Benson, F. E., Hewitt, R., Ford, K. J., Martin, F. L., Harriott, P., Cookson, M. R., and Allsop, D. (2004) A strategy for designing inhibitors of alpha-synuclein aggregation and toxicity as a novel treatment for Parkinson's disease and related disorders. *FASEB J. 18*, 1315−1317.

(13) Scrocchi, L. A., Chen, Y., Waschuk, S., Wang, F., Cheung, S., Darabie, A. A., McLaurin, J., and Fraser, P. E. (2002) Design of

peptide-based inhibitors of human islet amyloid polypeptide fibrillogenesis. *J. Mol. Biol. 318*, 697−706.
(14) Yan, L.-M., Tatarek-Nossol, M., Velkova, A., Kazantzis, A., and Kapurniotu, A. (2006) Design of a mimic of nonamyloidogenic and bioactive human islet amyloid polypeptide (IAPP) as nanomolar affinity inhibitor of IAPP cytotoxic fibrillogenesis. *Proc. Natl. Acad. Sci. U.S.A. 103*, 2046−2051.
(15) Potter, K. J., Scrocchi, L. A., Warnock, G. L., Ao, Z., Younker, M. A., Rosenberg, L., Lipsett, M., Verchere, C. B., and Fraser, P. E. (2009) Amyloid inhibitors enhance survival of cultured human islets. *Biochim. Biophys. Acta, Gen. Subj. 1790*, 566−574.
(16) Mazor, Y., Gilead, S., Benhar, I., and Gazit, E. (2002) Identification and characterization of a novel molecular-recognition and self-assembly domain within the islet amyloid polypeptide. *J. Mol. Biol. 322*, 1013−1024.
(17) Tartaglia, G. G., Cavalli, A., Pellarin, R., and Caflisch, A. (2005) Prediction of aggregation rate and aggregation-prone segments in polypeptide sequences. *Protein Sci. 14*, 2723−2734.
(18) Jones, S., Manning, J., Kad, N. M., and Radford, S. E. (2003) Amyloid-forming peptides from [beta]2-microglobulin–insights into the mechanism of fibril formation in vitro. *J. Mol. Biol. 325*, 249−257.
(19) Miller, Y., Ma, B., and Nussinov, R. (2011) Synergistic interactions between repeats in tau protein and Aβ amyloids may be responsible for accelerated aggregation via polymorphic states. *Biochemistry 50*, 5172−5181.
(20) Guo, J.-P., Arai, T., Miklossy, J., and McGeer, P. L. (2006) Aβ and tau form soluble complexes that may promote self aggregation of both into the insoluble forms observed in Alzheimer's disease. *Proc. Natl. Acad. Sci. U.S.A. 103*, 1953−1958.
(21) Andreetto, E., Yan, L.-M., Tatarek-Nossol, M., Velkova, A., Frank, R., and Kapurniotu, A. (2010) Identification of hot regions of the Aβ−IAPP interaction interface as high-affinity binding sites in both cross- and self-association. *Ange. Chem., Int. Ed. 49*, 3081−3085.
(22) Rezaei-Ghaleh, N., Andreetto, E., Yan, L.-M., Kapurniotu, A., and Zweckstetter, M. (2011) Interaction between amyloid beta peptide and an aggregation blocker peptide mimicking islet amyloid polypeptide. *PLoS One 6*, e20289.
(23) Seeliger, J., Evers, F., Jeworrek, C., Kapoor, S., Weise, K., Andreetto, E., Tolan, M., Kapurniotu, A., and Winter, R. (2012) Cross-amyloid interaction of Abeta and IAPP at lipid membranes. *Angew. Chem., Int. Ed. Engl. 51*, 679−683.
(24) Buxbaum, J. N., Ye, Z., Reixach, N., Friske, L., Levy, C., Das, P., Golde, T., Masliah, E., Roberts, A. R., and Bartfai, T. (2008) Transthyretin protects Alzheimer's mice from the behavioral and biochemical effects of Abeta toxicity. *Proc. Natl. Acad. Sci. U.S.A. 105*, 2681−2686.
(25) Giasson, B. I., Forman, M. S., Higuchi, M., Golbe, L. I., Graves, C. L., Kotzbauer, P. T., Trojanowski, J. Q., and Lee, V. M. (2003) Initiation and synergistic fibrillization of tau and alpha-synuclein. *Science 300*, 636−640.
(26) Jensen, P. H., Hager, H., Nielsen, M. S., Højrup, P., Gliemann, J., and Jakes, R. (1999) Alpha-synuclein binds to Tau and stimulates the protein kinase A-catalyzed tau phosphorylation of serine residues 262 and 356. *J. Biol. Chem. 274*, 25481−25489.
(27) Yu, X., Luo, Y., Dinkel, P., Zheng, J., Wei, G., Margittai, M., Nussinov, R., and Ma, B. (2012) Cross-seeding and conformational selection between three- and four-repeat human Tau proteins. *J. Biol. Chem. 287*, 14950−14959.
(28) Siddiqua, A., Luo, Y., Meyer, V., Swanson, M. A., Yu, X., Wei, G., Zheng, J., Eaton, G. R., Ma, B., Nussinov, R., Eaton, S. S., and Margittai, M. (2012) Conformational basis for asymmetric seeding barrier in filaments of three- and four-repeat tau. *J. Am. Chem. Soc. 134*, 10271−10278.
(29) Middleton, C. T., Marek, P., Cao, P., Chiu, C.-c., Singh, S., Woys, A. M., de Pablo, J. J., Raleigh, D. P., and Zanni, M. T. (2012) Two-dimensional infrared spectroscopy reveals the complex behaviour of an amyloid fibril inhibitor. *Nat. Chem. 4*, 355−360.
(30) Hu, R., Zhang, M., Patel, K., Wang, Q., Chang, Y., Gong, X., Zhang, G., and Zheng, J. (2014) Cross-sequence interactions between human and rat islet amyloid polypeptides. *Langmuir 30*, 5193−5201.
(31) Hartman, K., Brender, J. R., Monde, K., Ono, A., Evans, M. L., Popovych, N., Chapman, M. R., and Ramamoorthy, A. (2013) Bacterial curli protein promotes the conversion of PAP248−286 into the amyloid SEVI: Cross-seeding of dissimilar amyloid sequences. *PeerJ 1*, e5.
(32) Souza, J. M., Giasson, B. I., Lee, V. M., and Ischiropoulos, H. (2000) Chaperone-like activity of synucleins. *FEBS Lett. 474*, 116−119.
(33) Westermark, P., Li, Z. C., Westermark, G. T., Leckstrom, A., and Steiner, D. F. (1996) Effects of beta cell granule components on human islet amyloid polypeptide fibril formation. *FEBS Lett. 379*, 203−206.
(34) Gilead, S., Wolfenson, H., and Gazit, E. (2006) Molecular mapping of the recognition interface between the islet amyloid polypeptide and insulin. *Angew. Chem., Int. Ed. Engl. 45*, 6476−6480.
(35) Mazor, Y., Gilead, S., Benhar, I., and Gazit, E. (2002) Identification and characterization of a novel molecular-recognition and self-assembly domain within the islet amyloid polypeptide. *J. Mol. Biol. 322*, 1013−1024.
(36) Ma, B., and Nussinov, R. (2012) Selective molecular recognition in amyloid growth and transmission and cross-species barriers. *J. Mol. Biol. 421*, 172−184.
(37) Nelson, R., Sawaya, M. R., Balbirnie, M., Madsen, A. O., Riekel, C., Grothe, R., and Eisenberg, D. (2005) Structure of the cross-beta spine of amyloid-like fibrils. *Nature 435*, 773−778.
(38) Gazit, E. (2005) Mechanisms of amyloid fibril self-assembly and inhibition. *FEBS J. 272*, 5971−5978.
(39) Yan, L. M., Velkova, A., Tatarek-Nossol, M., Andreetto, E., and Kapurniotu, A. (2007) IAPP mimic blocks Abeta cytotoxic self-assembly: cross-suppression of amyloid toxicity of Abeta and IAPP suggests a molecular link between Alzheimer's disease and type II diabetes. *Angew. Chem., Int. Ed. Engl. 46*, 1246−1252.
(40) Gilead, S., and Gazit, E. (2004) Inhibition of amyloid fibril formation by peptide analogues modified with alpha-aminoisobutyric acid. *Angew. Chem., Int. Ed. Engl. 43*, 4041−4044.
(41) Gazit, E. (2005) Mechanisms of amyloid fibril self-assembly and inhibition. Model short peptides as a key research tool. *FEBS J. 272*, 5971−5978.
(42) Liang, G., Liu, Y., Shi, B., Zhao, J., and Zheng, J. (2013) An index for characterization of natural and non-natural amino acids for peptidomimetics. *PLoS One 8*, e67844.
(43) Maurer-Stroh, S., Debulpaep, M., Kuemmerer, N., Lopez de la Paz, M., Martins, I. C., Reumers, J., Morris, K. L., Copland, A., Serpell, L., Serrano, L., Schymkowitz, J. W. H., and Rousseau, F. (2010) Exploring the sequence determinants of amyloid structure using position-specific scoring matrices. *Nat. Methods 7*, 237−242.
(44) Thompson, M. J., Sievers, S. A., Karanicolas, J., Ivanova, M. I., Baker, D., and Eisenberg, D. (2006) The 3D profile method for identifying fibril-forming segments of proteins. *Proc. Natl. Acad. Sci. U.S.A. 103*, 4074−4078.
(45) Goldschmidt, L., Teng, P. K., Riek, R., and Eisenberg, D. (2010) Identifying the amylome, proteins capable of forming amyloid-like fibrils. *Proc. Natl. Acad. Sci. U.S.A. 107*, 3487−3492.
(46) Kale, L., Skeel, R., Bhandarkar, M., Brunner, R., Gursoy, A., Krawetz, N., Phillips, J., Shinozaki, A., Varadarajan, K., and Schulten, K. (1999) NAMD2: greater scalability for parallel molecular dynamics. *J. Comput. Phys. 151*, 283−312.
(47) MacKerell, A. D., Bashford, D., Bellott, M., Dunbrack, R. L., Evanseck, J. D., Field, M. J., Fischer, S., Gao, J., Guo, H., Ha, S., Joseph-McCarthy, D., Kuchnir, L., Kuczera, K., Lau, F. T. K., Mattos, C., Michnick, S., Ngo, T., Nguyen, D. T., Prodhom, B., Reiher, W. E., Roux, B., Schlenkrich, M., Smith, J. C., Stote, R., Straub, J., Watanabe, M., Wiorkiewicz-Kuczera, J., Yin, D., and Karplus, M. (1998) All-atom empirical potential for molecular modeling and dynamics studies of proteins. *J. Phys. Chem. B 102*, 3586−3616.

(48) Cairo, C. W., Strzelec, A., Murphy, R. M., and Kiessling, L. L. (2002) Affinity-based inhibition of beta-amyloid toxicity. *Biochemistry 41*, 8620−8629.
(49) Maurer-Stroh, S., Debulpaep, M., Kuemmerer, N., Lopez de la Paz, M., Martins, I. C., Reumers, J., Morris, K. L., Copland, A., Serpell, L., Serrano, L., Schymkowitz, J. W., and Rousseau, F. (2010) Exploring the sequence determinants of amyloid structure using position-specific scoring matrices. *Nat. Methods 7*, 237−242.
(50) Chou, K. C., and Shen, H. B. (2007) Recent progress in protein subcellular location prediction. *Anal. Biochem. 370*, 1−16.
(51) Nelson, R., Sawaya, M. R., Balbirnie, M., Madsen, A. O., Riekel, C., Grothe, R., and Eisenberg, D. (2005) Structure of the cross-beta spine of amyloid-like fibrils. *Nature 435*, 773−778.
(52) Wang, Q., Shah, N., Zhao, J., Wang, C., Zhao, C., Liu, L., Li, L., Zhou, F., and Zheng, J. (2011) Structural, morphological, and kinetic studies of beta-amyloid peptide aggregation on self-assembled monolayers. *Phys. Chem. Chem. Phys. 13*, 15200−15210.
(53) Wang, Q. M., Yu, X., Patal, K., Hu, R. D., Chuang, S., Zhang, G., and Zheng, J. (2013) Tanshinones Inhibit Amyloid Aggregation by Amyloid-beta Peptide, Disaggregate Amyloid Fibrils, and Protect Cultured Cells. *ACS Chem. Neurosci. 4*, 1004−1015.